

Fast, Accurate and Object Boundary-Aware Surface Normal Estimation from Depth Maps

Saed Moradi

Computer Vision and Systems Laboratory (CVSL)
Laval University Quebec, QC G1V0A6, Canada

Alireza Memarmoghadam

Department of Electrical Engineering
University of Isfahan, Isfahan, Iran

Denis Laurendeau

Computer Vision and Systems Laboratory (CVSL)
Laval University Quebec, QC G1V0A6, Canada

Abstract

This paper proposes a fast and accurate surface normal estimation method which can be directly used on depth maps (organized point clouds). The surface normal estimation process is formulated as a closed-form expression. In order to reduce the effect of measurement noise, the averaging operation is utilized in multi-direction manner. The multi-direction normal estimation process is reformulated in the next step to be implemented efficiently. Finally, a simple yet effective method is proposed to remove erroneous normal estimation at depth discontinuities. The proposed method is compared to well-known surface normal estimation algorithms. The results show that the proposed algorithm not only outperforms the baseline algorithms in term of accuracy, but also is fast enough to be used in real-time applications.

1. Introduction

Surface normal vectors estimation [7, 3, 14] is the common process in different 3D vision and 3D processing task such as 3D surface reconstruction [10], scene segmentation [13], object recognition [16], and others. A complete 3D processing pipeline may fail due to lack of effective surface normal estimation process. Thus, fast and accurate normal estimation is of great importance in practical application. There are several approaches dedicated to normal estimation in the literature depending on the type of input 3D data. For an unorganized point clouds (an unordered set of 3D points), at the first step, a graph should be constructed to identify the neighboring points for each query points. Then, the vector normal to the query point is estimated. The most common approach for surface normal estimation is called plane-PCA ([1]). In this method, a plane is fitted to the

all neighboring points (including the query point). Then, the vector normal to the fitted plane is determined by eigen decomposition of the scattering matrix. The eigen vector correspond to the smallest eigen value is considered as the surface normal vector. The plane-PCA method is a robust and accurate method. However, it is not suitable for large-scale point clouds due to its high computational complexity. Beside the plane-PCA, too many research have been done to improve the accuracy of the surface normal estimation process.

In [8], in order to improve the normal estimation accuracy for points belonging to high curvature surfaces, an optimum tangent plane is fitted using robust statistics. Randomized Hough Transform (RHT) along with statistical exploration bounds is used to preserve sharp features in [2]. To reduce the computational complexity, the authors used a fixed-size accumulator. A GPU-based implementation is proposed in [9] to speed-up a computationally intensive tensor voting algorithm. In order to exclude the outliers, the Deterministic MM-estimator (DetMM) is used in [6]. In addition to classical data processing techniques, deep learning-based methods have recently attracted the attention of the research community for surface normal vector estimation [7, 17]. However, these methods usually require richly labeled datasets.

Comparing to unorganized point clouds, surface normal estimation directly from a depth map (organized point cloud) has received less attention in the literature. However, estimating surface normal from depth maps has the following advantages:

- No extra processing step is needed to determine the points belonging to the neighborhood of a query point.
- The complete normal estimation process can be implemented through 2D image processing operators which are much faster than 3D ones.

Some research in the literature focuses on the estimation of normal vectors directly from input depth images. In [15] a closed-form expression is proposed for estimating normal vectors at each point. However, improper tangent vector selection led to inaccurate normals map. Holzer et al. [5] proposed a surface normal estimation method based on adaptive neighboring size selection and integral images. However, the accuracy of their method depends on hyper-parameters values which are chosen empirically. Also, the performance of their method is degraded facing small objects with high surface curvature. One of the most accurate and fast surface normal estimation methods is presented in [12]. While the surface tangent vectors are constructed perfectly, the approximation error of first-order partial derivatives decreases the accuracy of the estimation process. Authors in [4] proposed a fast and accurate method for surface normal estimation. The method is also implemented using GPU to achieve higher performance. Despite the superiority of the method, the method is unable to estimate normal vectors for uniform areas. In our previous work [11], a fast and accurate surface normal estimation method is proposed. In that work, a closed-form expression is proposed for each component of the surface normal vectors. Also, the method is capable of multi-scale implementation which in turn decreases the effect of the measurement noise. However, using multi-scale approach increases the execution time of the algorithm. To address this issue, a fast and accurate surface normal estimation method is presented in this paper. The contributions of this work are as follows:

1. The averaging process in multi-scale approach is used in multi-direction manner to suppress the effect of measurement noise.
2. The multi-direction method is implemented in an efficient manner.
3. The erroneous estimated normal vectors are excluded from final normal map using a simple yet effective method.

The rest of this paper is organized as follows: In section 2, our previous work is reviewed briefly as motivation to current work. In section 3 the proposed method is explained in details. Section 4 is dedicated to experiments and results. Finally, the paper is concluded in section 5.

2. Motivation and Background

In our previous work [11], a fast method was proposed to estimate surface normal vectors directly from depth maps. In this work, first, the projection of two surface tangent vectors in the depth map is constructed (Figure 1). Then, the cross product of these two tangent vectors is considered as

the surface normal vector at the query point. The closed-form solution for the normal vectors were derived as follows:

$$n_x = -\frac{\alpha}{f_y} d_3 (d_2 - d_1) \quad (1)$$

$$n_y = -\frac{\alpha}{f_x} d_2 (d_3 - d_1) \quad (2)$$

$$n_z = \frac{\alpha}{f_x} v_1 d_2 (d_3 - d_1) + \frac{\alpha}{f_y} u_1 d_3 (d_2 - d_1) + \frac{\alpha^2}{f_x f_y} d_2 d_3 \quad (3)$$

where, f_x and f_y denote the focal lengths. Also, $d_i = g(r_i, c_i)$, $u_i = \frac{r_i - o_x}{f_x}$, $v_i = \frac{c_i - o_y}{f_y}$. o_x and o_y are the coordinates of the optical center.

In case of noisy input, the averaging process on multi-scale results will reduce the effect of noise. Therefore:

$$n_x = \frac{-1}{K} \sum_{i=1}^K \frac{\alpha_i}{f_y} d_3 (d_2 - d_1) \quad i = 1, 2, \dots, K \quad (4)$$

$$n_y = \frac{-1}{K} \sum_{i=1}^K \frac{\alpha_i}{f_x} d_2 (d_3 - d_1) \quad i = 1, 2, \dots, K \quad (5)$$

$$n_z = \frac{1}{K} \sum_{i=1}^K \frac{\alpha_i}{f_x} v_1 d_2 (d_3 - d_1) + \frac{\alpha_i}{f_y} u_1 d_3 (d_2 - d_1) + \frac{\alpha_i^2}{f_x f_y} d_2 d_3 \quad i = 1, 2, \dots, K \quad (6)$$

While the single-scale version of this method is fast and gives an accurate estimation of normal vectors for smooth surfaces, the multi-scale normal estimation is slower by a factor equal to the number of scales. Moreover, the effect of depth discontinuity at object boundaries is not considered. In the next section, both shortcomings of our previous work are addressed and a fast, accurate, and object

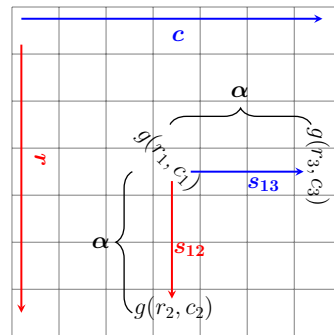


Figure 1: 2D projection of surface tangent vectors on the depth map [11].

boundary-aware surface normal vector estimation method is presented.

3. The Proposed Method

3.1. Fast normal estimation

In our previous work [11], a multi-scale approach is used to reduce the effect of measurement noise on the final estimated surface normal vectors. The averaging operation among different scales can effectively reduce the noise effect. However, using K scales for final normal construction increases the execution time by a factor of K compared to the single-scale approach. In order to benefit from averaging operation in noise effect reduction, here, we use multiple pairs of different tangent vectors to estimate the surface normal at a query point. Then, the final normal vector at each point is obtained by taking the average value of the resulting normal vectors. Figure 2 shows the projection of four different surface tangent vectors on depth maps. While, the cross product of every vectors pair can be used to estimate the normal vectors, only perpendicular tangent vectors pairs are considered, here. The average value of all resulting normal vectors is the final normal vector for each query point. The averaging process makes this estimation robust against measurement noise.

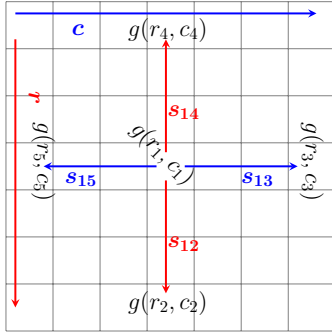


Figure 2: Projection of surface tangent vectors construction in all four main directions

Considering all four tangent vector pairs, the normal vector can be estimated as:

$$\begin{aligned}
 n &= 0.25(n_{23} + n_{34} + n_{45} + n_{52}) \\
 &= 0.25(s_{12} \times s_{13} + s_{13} \times s_{14} + s_{14} \times s_{15} + s_{15} \times s_{12}) \\
 &= 0.25(s_{12} \times s_{13} - s_{14} \times s_{13} + s_{14} \times s_{15} - s_{12} \times s_{15}) \\
 &= 0.25(s_{12} - s_{14}) \times s_{13} + (s_{14} - s_{12}) \times s_{15} \\
 &= 0.25(s_{12} - s_{14}) \times s_{13} - (s_{12} - s_{14}) \times s_{15} \\
 &= 0.25((s_{12} - s_{14}) \times (s_{13} - s_{15})) \\
 &= 0.25(s_{24} \times s_{35})
 \end{aligned} \tag{7}$$

where, s_{24} and s_{35} are two tangent vectors which are depicted in Figure 3. Equation 7 proves that the result of the summation of four different cross products can be achieved using a single cross product. This means that using this approach can accelerate the normal estimation process by a factor of 4. Finally, the closed-form solution for the normal vectors can be determined as:

$$s_{24} = \begin{bmatrix} x_4 - x_2 \\ y_4 - y_2 \\ z_4 - z_2 \end{bmatrix} = \begin{bmatrix} u_4 d_4 - u_2 d_2 \\ v_4 d_4 - v_2 d_2 \\ d_4 - d_2 \end{bmatrix} \tag{8}$$

$$s_{35} = \begin{bmatrix} x_5 - x_3 \\ y_5 - y_3 \\ z_5 - z_3 \end{bmatrix} = \begin{bmatrix} u_5 d_5 - u_3 d_3 \\ v_5 d_5 - v_3 d_3 \\ d_5 - d_3 \end{bmatrix} \tag{9}$$

$$n_x = -\frac{\alpha}{4f_y} (d_3 + d_5) (d_2 - d_4) \tag{10}$$

$$n_y = -\frac{\alpha}{4f_x} (d_2 + d_4) (d_3 - d_5) \tag{11}$$

$$n_z = -u_1 n_x - v_1 n_y + \frac{\alpha^2}{4f_x f_y} (d_2 + d_4) (d_3 + d_5) \tag{12}$$

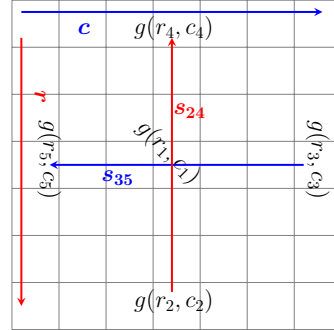


Figure 3: Projection of final surface tangent vectors

3.2. Considering object boundaries

The proposed method as well as our previous work [11] works well when facing the points belonging to surfaces without depth discontinuances. However, at the object boundaries, at least one of the surface tangent vectors is not valid. Therefore, the orientation of the estimated normal vector may be erroneous. To tackle this problem, a new approach is presented here.

Surface normals are unit vectors and their orientations are the only important parameters in 3D processing. This is why only ϕ and θ components are taken into account when a normal vector is converted from Cartesian coordinates into spherical one. However, the length of estimated normal vector depends on the length of tangent vectors as follows:

$$\|n\|_2 \propto \|s_{24} \times s_{35}\|_2 \propto \|s_{24}\|_2 \cdot \|s_{35}\|_2 \tag{13}$$

Since at least one of the tangent vectors has a large length in object boundaries, Equation 13 indicates that the length of the normal also should be large in those areas. Thus, the length of the vector (r component in spherical coordinates) can be used as a mask to find and exclude erroneous normal estimation. A simple thresholding on r values gives the location of outliers. The final normal estimation is performed by applying the invalid points mask to the estimated normal map.

4. Experimental results

In order to evaluate the normal estimation performance of the proposed method, experiments were carried out on real data captured by a Microsoft Kinect Azure RGB-D camera as well as synthetic depth from 3F2N [4] dataset. All the algorithms are implemented in MATLAB. The full specifications of implementation environment are reported in Table 1.

There are two ways to demonstrate a surface normal vector as an image. In the first one, each component of the normal vector is considered as a color channel and the resulting vector from depth map can be treated as a color image. While this way is straightforward, it can not highlight small errors in the estimated normal vectors. The second way is to convert the normal vector to spherical coordinates and investigate I_ϕ and I_θ components. I_ϕ and I_θ can be calculated as:

$$I_\phi = \tan^{-1} \left(\frac{n_y}{n_x} \right) \quad (14)$$

$$I_\theta = \tan^{-1} \left(\frac{\sqrt{n_x^2 + n_y^2}}{n_z} \right) \quad (15)$$

The results of I_θ and I_ϕ for different real depth maps are depicted in Figure 4 and Figure 5, respectively. As shown in these figures, the proposed method outperforms all the baseline algorithms in term of similarity to the ground truth images. The second place belongs to our previous work [11]. In order to have a fair comparison, the α value for both algorithms is set to 2. Also, the results of the plane fitting-based method with 25 neighboring points are considered as ground truths. Figure 6 and Figure 7 show the result of normal estimation on 3F2N dataset. Again, the proposed method and our previous work outperform the other works. Since, the synthetic images are smooth enough, the Nakagawa’s method does not affected by sensitivity of partial derivatives to noise. This is why this method performs well on synthetic data compared to real data.

For quantitative comparison, the Mean Squared error (MSE) is used as the performance metric. Table 2, Table 3, Table 4, and Table 5 show the MSE values of both θ and ϕ image components. As reported in the tables, the proposed method shows the best performance among all the

Table 1: The full specifications of the implementation environment

Operating System	Ubuntu 20.04
MATLAB version	2021b
Size of the test image	576×640
data type	double precision 64 bit floating point
CPU	Intel CORE i7-3520M @ 2.90GHz
Memory	16GB DDR3 @ 1600MHz

Table 2: Mean Squared error (MSE) of I_θ images

	[5]	[12]	[4]	[11]	ours
1 st scene	3.2845	2.4227	1.8098	1.0161	0.9301
2 nd scene	2.9482	2.3099	1.3769	1.0783	0.9150
3 rd scene	2.6559	2.6072	1.2687	1.0244	0.8032
4 th scene	2.8190	2.7241	1.2618	1.0012	0.8918

Table 3: Mean Squared error (MSE) of I_ϕ images

	[5]	[12]	[4]	[11]	ours
1 st scene	1.8521	5.2841	1.9734	1.8842	1.6655
2 nd scene	2.0199	5.1293	2.0401	2.0785	1.7884
3 rd scene	2.0313	5.1036	2.1251	2.0288	1.7738
4 th scene	2.2078	4.8315	2.2550	2.1463	1.9697

Table 4: Mean Squared error (MSE) of I_θ images (3F2N dataset [4])

	[12]	[4]	[11]	ours
1 st scene	0.0790	3.3966	0.0779	0.0491
2 nd scene	0.2408	2.8881	0.2378	0.1333
3 rd scene	0.1414	0.7437	0.1415	0.1465
4 th scene	0.8808	0.7672	0.8852	0.6874

Table 5: Mean Squared error (MSE) of I_ϕ images (3F2N dataset [4])

	[12]	[4]	[11]	ours
1 st scene	0.0363	0.0616	0.0363	0.0616
2 nd scene	0.0422	0.0517	0.0422	0.0517
3 rd scene	0.1259	0.1411	0.1259	0.1411
4 th scene	0.1935	0.2142	0.1937	0.2143

baseline algorithms except for the ϕ component of the synthetic depth images which there is not a significant difference among all the baseline algorithms. Since the synthetic data are relatively smooth, the α value for the proposed method as well as our previous work [11] is set to 1. In this situation, Nakagawa’s method shows same behavior as our previous work (Table 4 and and Table 5). Note that all images are normalized in $[0 - 2\pi]$ range.

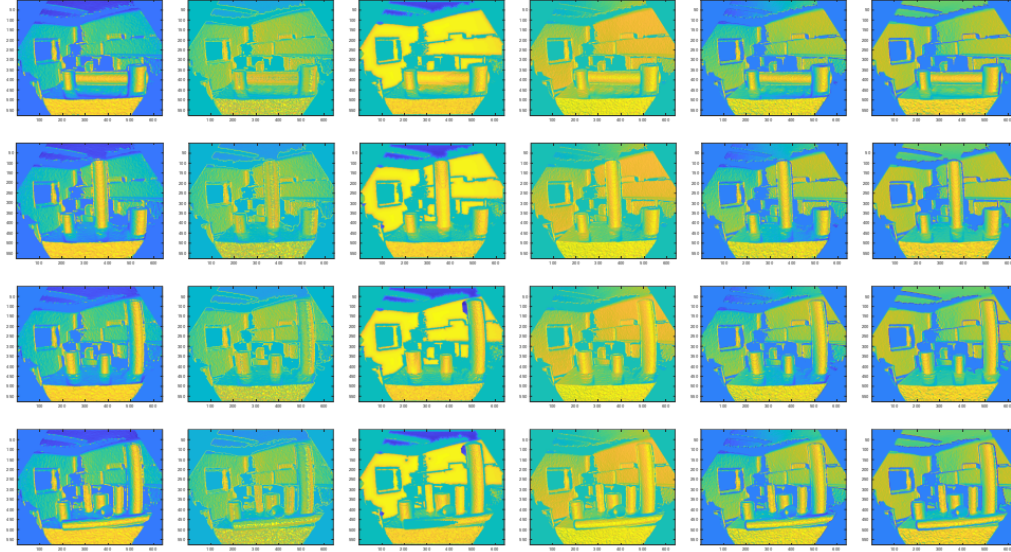


Figure 4: I_θ images of the estimation results of different algorithms (Real images). From left: the ground truth, Fan's method [4], Holzer's method [5], Nakagawa's method [12], Moradi's method [11], **the proposed method**.

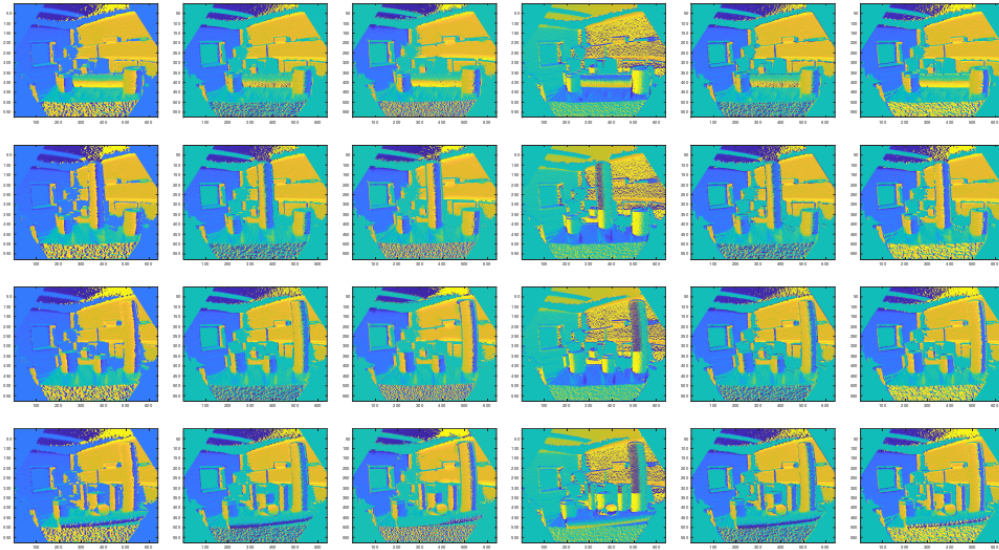


Figure 5: I_ϕ images of the estimation results of different algorithms (Real images). From left: the ground truth, Fan's method [4], Holzer's method [5], Nakagawa's method [12], Moradi's method [11], **the proposed method**.

The color image representation of normal vectors can be used to demonstrate the erroneous surface normal estimation at object boundaries. Figure 8 shows the invalid normal vectors removal operation, step by step. Fig. Figure 8a shows the estimated surface normal vectors using Equation 7. As shown in this figure, there are some erroneous estimation at the locations with the depth discontinuity. As mentioned in subsection 3.2, the large values of r component (Fig. Figure 8b) in spherical coordinates have a high potential to be the erroneous estimation. A simple

thresholding on r values gives the location of outliers (Fig. Figure 8c). The final normal estimation is performed by applying the mask in Fig. Figure 8c to Fig. Figure 8a. Fig. Figure 8d shows the final result of surface normal estimation.

Finally, in order to evaluate the running time of the baseline algorithms as well as the proposed one, all the algorithms are implemented in the MATLAB environment (The MATLAB implementation of the 3F2N method is available in their github repository [4]). Each algorithm is executed

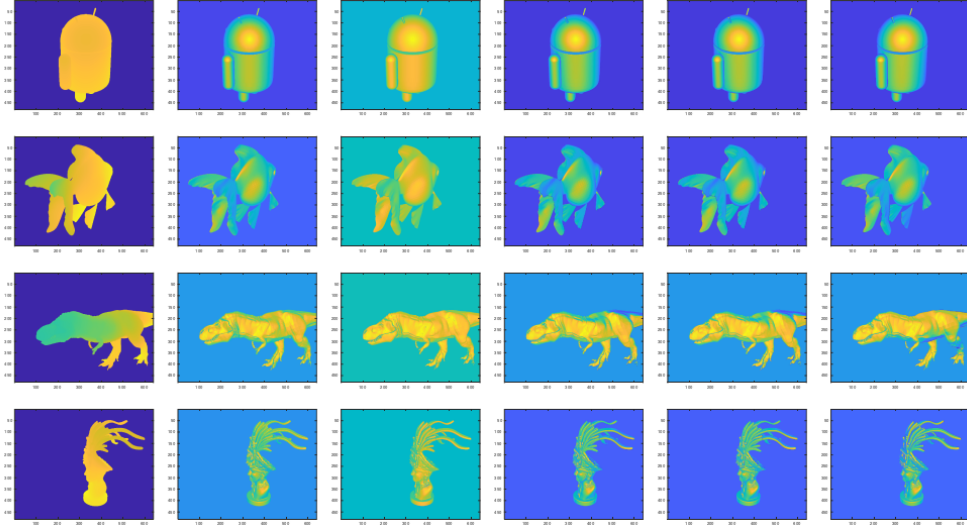


Figure 6: I_θ images of the estimation results of different algorithms (Synthetic images from 3F2N dataset [4]). From left: the depth image, ground truth, Fan’s method [4], Nakagawa’s method [12], Moradi’s method [11], **the proposed method**.

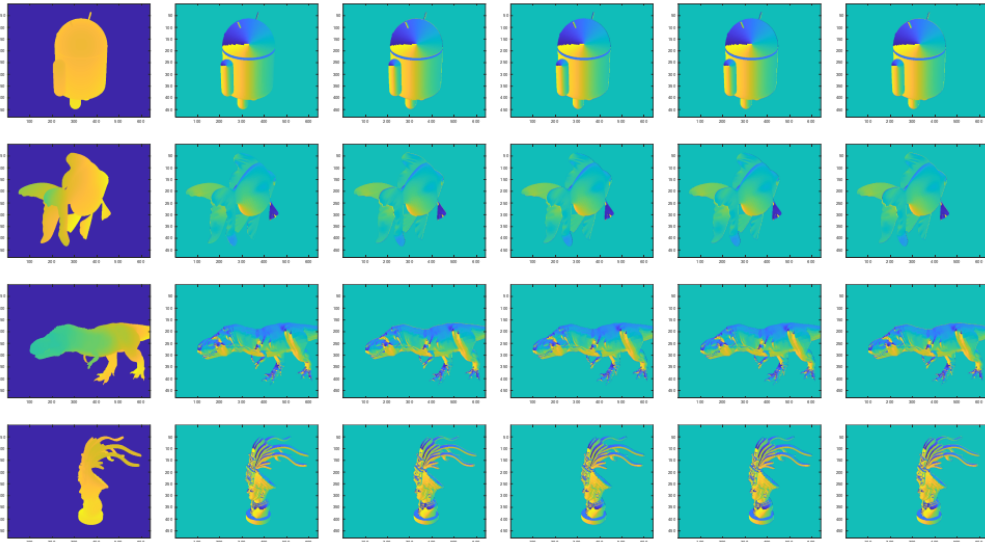


Figure 7: I_ϕ images of the estimation results of different algorithms (Synthetic images from 3F2N dataset [4]). From left: the depth image, ground truth, Fan’s method [4], Nakagawa’s method [12], Moradi’s method [11], **the proposed method**.

200 times and the average running times are reported in Table 6. As reported in the table, the proposed method ranked in second place after Moradi’s method (our previous work) [11]. The proposed method is slightly slower than our previous work. Note that, a single scale implementation of the proposed method is equivalent to four scales implementation of our previous work. Thus, this work is almost four times faster than our previous work. The normal estimation process can be performed in 135 fps using the proposed method. Fan’s method has a straightforward implementa-

tion. However, searching for invalid points ($\Delta Z = 0$) in the normal map increases the execution time of this method.

5. Conclusion

In this paper an improved version of our previous work is presented. In our previous work, the normal estimation process is formulated as a closed-form solution which was efficiently implemented. However, multi-scale implementation is necessary for tackling measurement noise which in turn leads to lower computational efficiency. In this work,

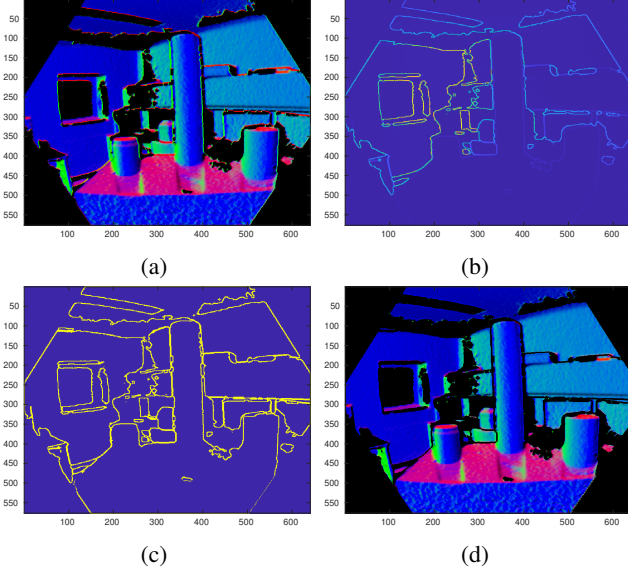


Figure 8: Surface normal vectors refinement at object boundaries. a) initial surface normal estimation using Equation 7, b) value of r component for each point, c) outlier removal mask, and d) final result of surface normal estimation

Table 6: The average execution time for different normal estimation methods for a 576×640 depth image

Estimation method	execution time (mS)
local plane fitting	3776
Holzer’s method [5]	804.620
Nakagawa’s method [12]	17.132
Fan’s method [4]	154.676
Moradi’s method [11]	6.646
The proposed method	7.415

instead of changing the pixel distance value parameter α the averaging process is adopted for different directions to reduce the effects of the measurement noise. Next, the multi-direction approach is reformulated so that it can be efficiently implemented. So far, the proposed normal estimation method is fast and accurate for smooth surfaces. However, it produces erroneous results when facing object boundaries and depth discontinuities. To address this issues, a simple yet effective mask is constructed based on the length of the estimated normal vectors. This mask is used to exclude erroneous normal vectors from final normal map. The proposed method is compared to some well-known surface normal estimation algorithms. Qualitative and quantitative comparisons on real as well as synthetic depth images show that the proposed surface normal estimation method outperforms the baseline algorithms in both terms of accuracy and computational complexity.

References

- [1] Jens Berkmann and Terry Caelli. Computation of surface geometry and segmentation using covariance techniques. *IEEE Transactions on Pattern Analysis and Machine Intelligence*, 16(11):1114–1116, 1994.
- [2] Alexandre Boulch and Renaud Marlet. Fast and robust normal estimation for point clouds with sharp features. In *Computer graphics forum*, volume 31, pages 1765–1774. Wiley Online Library, 2012.
- [3] Tien Do, Khiem Vuong, Stergios I Roumeliotis, and Hyun Soo Park. Surface normal estimation of tilted images via spatial rectifier. In *European Conference on Computer Vision*, pages 265–280. Springer, 2020.
- [4] Rui Fan, Hengli Wang, Bohuan Xue, Huaiyang Huang, Yuan Wang, Ming Liu, and Ioannis Pitas. Three-filters-to-normal: An accurate and ultrafast surface normal estimator. *IEEE Robotics and Automation Letters*, 6(3):5405–5412, 2021.
- [5] Stefan Holzer, Radu Bogdan Rusu, Michael Dixon, Suat Gedikli, and Nassir Navab. Adaptive neighborhood selection for real-time surface normal estimation from organized point cloud data using integral images. In *2012 IEEE/RSJ International Conference on Intelligent Robots and Systems*, pages 2684–2689. IEEE, 2012.
- [6] Ali Khaloo and David Lattanzi. Robust normal estimation and region growing segmentation of infrastructure 3d point cloud models. *Advanced Engineering Informatics*, 34:1–16, 2017.
- [7] Jan Eric Lenssen, Christian Osendorfer, and Jonathan Masci. Deep iterative surface normal estimation. In *Proceedings of the IEEE/CVF Conference on Computer Vision and Pattern Recognition*, pages 11247–11256, 2020.
- [8] Bao Li, Ruwen Schnabel, Reinhard Klein, Zhiquan Cheng, Gang Dang, and Shiyao Jin. Robust normal estimation for point clouds with sharp features. *Computers & Graphics*, 34(2):94–106, 2010.
- [9] Ming Liu, François Pomerleau, Francis Colas, and Roland Siegwart. Normal estimation for pointcloud using gpu based sparse tensor voting. In *2012 IEEE International Conference on Robotics and Biomimetics (ROBIO)*, pages 91–96. IEEE, 2012.
- [10] Dening Lu, Xuequan Lu, Yangxing Sun, and Jun Wang. Deep feature-preserving normal estimation for point cloud filtering. *Computer-Aided Design*, 125:102860, 2020.
- [11] Saed Moradi, Denis Laurendeau, and Clement Gosselin. Multiple cylinder extraction from organized point clouds. *Sensors*, 21(22):7630, 2021.
- [12] Yosuke Nakagawa, Hideaki Uchiyama, Hajime Nagahara, and Rin-Ichiro Taniguchi. Estimating surface normals with depth image gradients for fast and accurate registration. In *2015 International Conference on 3D Vision*, pages 640–647. IEEE, 2015.
- [13] Florent Poux, Christian Mattes, and Leif Kobbelt. Unsupervised segmentation of indoor 3d point cloud: application to object-based classification. *International Archives of the Photogrammetry, Remote Sensing and Spatial Information Sciences*, 44(W1-2020):111–118, 2020.

- [14] Ja-Won Seo, Kyung-Eun Kim, and Kyungshik Roh. 3d hole center and surface normal estimation in robot vision systems. In *2020 IEEE/SICE International Symposium on System Integration (SII)*, pages 355–359. IEEE, 2020.
- [15] Shuai Tang, Xiaoyu Wang, Xutao Lv, Tony X Han, James Keller, Zhihai He, Marjorie Skubic, and Shihong Lao. Histogram of oriented normal vectors for object recognition with a depth sensor. In *Asian conference on computer vision*, pages 525–538. Springer, 2012.
- [16] Huan Zhao, Minjie Tang, and Han Ding. Hoppf: A novel local surface descriptor for 3d object recognition. *Pattern Recognition*, 103:107272, 2020.
- [17] Jun Zhou, Wei Jin, Mingjie Wang, Xiuping Liu, Zhiyang Li, and Zhaobin Liu. Improvement of normal estimation for pointclouds via simplifying surface fitting. *arXiv preprint arXiv:2104.10369*, 2021.